Mol Neurobiol (2016) 53:3576–3585
DOI 10.1007/s12035-015-9302-3

Effect Comparison of Both Iron Chelators on Outcomes, Iron Deposit, and Iron Transporters After Intracerebral Hemorrhage in Rats

Gaiqing Wang[1] · Weimin Hu[1] · Qingping Tang[2] · Li Wang[1] · Xin-gang Sun[1] · Yanli Chen[1] · Yongfeng Yin[1] · Fang Xue[1] · Zhitang Sun[1]

Received: 18 May 2015 / Accepted: 9 June 2015 / Published online: 23 June 2015

Abstract Iron overload plays a key role in brain injury after intracerebral hemorrhage (ICH). We explored the roles of ferric iron chelator—deferiprone (DFP)—and ferrous iron chelator—clioquinol (CQ)—in ICH rats through the outcomes, iron deposits, reactive oxygen species (ROS), brain water content, and related iron transporters. One hundred eight Sprague-Dawley rats received intra-striatal infusions of 0.5 U of type IV collagenase to establish ICH models. The rats were randomly assigned to the sham, vehicle, DFP, and CQ groups. We evaluated the outcomes, iron levels, brain water content, and ROS; meanwhile, immunohistochemistry and real-time quantitative polymerase chain reaction (RT-qPCR) were utilized to determine ferritin, transferrin, transferrin receptor, divalent metal transport 1 (DMT1), and ferroportin at 48 and 72 h, 7 and 14 days after surgery. Our results showed ICH induced iron overload, brain edema, ROS formation, and neurological deficits. Both iron chelators decreased iron levels; CQ improved the neurological outcome, attenuated brain edema, and ROS production. DFP reduced iron contents but not brain water content and ROS generation. DFP failed to improve the outcome. ICH initiated endogenous iron chelators and transporters, both exogenous iron chelators enhanced expression of transferrin and transferrin receptor. CQ enhanced expression of ferroportin but not DMT1, while DFP enhanced expression of DMT1 but not ferroportin. Ferrous iron contributed to brain injury, and binding ferrous iron can modestly improve outcome after ICH in rats. The exogenous ferrous iron chelator possibly functioned via endogenous ferrous iron transporters on ICH. Therefore, ferrous iron may be a promising target for ICH in future.

Keywords Intracerebral hemorrhage · Secondary brain injury · Iron deposit · Deferiprone · Clioquinol · Iron transporters

Introduction

Spontaneous intracerebral hemorrhage (ICH) is a common and fatal stroke subtype. Brain injury induced by ICH initially occurs within the first few hours as a result of mass effect due to hematoma formation. However, many patients continue to deteriorate clinically despite no signs of rebleeding or hematoma expansion. This continued insult after primary hemorrhage is believed to be mediated by the cytotoxic, excitotoxic, oxidative, and inflammatory effects of intraparenchymal blood [1]. Blood lysis starts at 24 h and continues for the next several days, leading to the release of cytotoxic hemoglobin (Hb) with further deterioration of the pathological status quo [2]. Iron, a major hemoglobin degradation product which accumulates in the brain parenchyma for months, has a detrimental effect in secondary injury [3–7]. Iron plays a key role in edema formation and cell death after ICH [5, 8]. Prominently, the mechanism of iron toxicity includes generating free radicals (mainly through Fenton-type mechanism) and directly compromising the neighboring brain cells. Reactive oxygen species (ROS) can directly or indirectly damage all biomolecules, including proteins, lipids, deoxyribonucleic acid (DNA), and carbohydrates [9]. So after ICH, the endogenous pathway for iron chelation and trafficking initiated to remove iron then reduce more damage in the brain.

✉ Gaiqing Wang
wanggq08@126.com

[1] Department of Neurology, the Second Hospital, Shanxi Medical University, 382 Wuyi Avenue, Taiyuan, Shanxi 030001, China

[2] Department of Rehabilitation, Brain Hospital of Hunan Province, 2427 Furong Middle Road, Changsha, Hunan 410007, China

Therefore, finding means of controlling absorption of iron and facilitating iron clearance may have important clinical implications. Therefore, exogenous iron chelation therapy seems to be a logical approach to remove toxic levels of iron. Deferoxamine, a ferric iron chelator, which is the most popular treatment in experimental intervention strategy in ICH, has been shown to mitigate iron-mediated damage [3, 4]. Unfortunately, recent data showed that deferoxamine can reduce the iron contents in the brain, but could not attenuate injury and improve neurological outcome [10, 11]. Deferiprone, another ferric iron chelator, because of its easy taking, stability, lipophilicity, high tissue penetration, and clearance of the iron complex, can be used as a potent pharmaceutical alternative therapy, especially in conditions when other treatments failed [12, 13]. Clioquinol, a ferrous iron chelator, is also known as metal-protein-attenuating compounds. The lipophilic nature of clioquinol allows for its effective use at lower concentrations [14].

In the experiment, we used deferiprone and clioquinol to intervene with ICH, observe the outcomes, iron levels, reactive oxygen species content, and iron transporters following ICH in rats, and compare the roles of deferiprone to clioquinol in ICH.

Materials and Methods

Animals

One hundred eight Sprague-Dawley male rats (250–300 g, 12 weeks old; obtained from the Animal Experimental Center and approved by the responsible Animal Care and Use Committee of Shanxi Medical University) were used in this study. Rats were given free access to food and water throughout the study.

Experimental Groups and Tissue Preparation

There were four groups in the experiment. Group A: sham group (n=24); group B: vehicle group (n=24); group C: deferiprone (Apotex Inc, Canada) in low dosage (125 mg/kg/day, n=24) and high dosage (200 mg/kg/day, n=6) group (n=30); group D: clioquinol (Wuhan Hong Xinkang Fine Chemical Engineering, China) in low dosage (50 mg/kg/day, n=6) and high dosage (100 mg/kg/day, n=24) group (n=30). Animals were randomly assigned to these groups. All gavages were administered intragastrically 24 h after ICH and twice a day until the euthanasia point.

When animals were sacrificed, the brains were removed and sectioned coronally into half from the surgery point. The half was continually sectioned into 3 mm slices and fixed with 4 % paraformaldehyde in 0.1 M phosphate buffer at 4 °C overnight, then passed through a grade series of sucrose in 0.1 M phosphate buffer and paraffin embedded ready for slice staining. The other coronary half brain was cut into right and left sides, and then put into the nitrogen, stored in −80 °C for brain water content, total iron content, ROS measurement, and real-time quantitative polymerase chain reaction (RT-qPCR).

Intracerebral Hemorrhage and Intervention Modeling

The rats were anesthetized using chloral hydrate (300–350 mg/kg intraperitoneally) and were placed in a stereotactic head frame (Jiangwan Instrument, Shanghai). A 1-mm cranial bur hole was then drilled on the right coronal suture 2.3 mm lateral to the midline. Then, 2 ul of saline containing 0.5 U of bacterial collagenase type IV (Sigma-Aldrich Co, USA) was injected into the right striatum (coordinates: 0.5 mm anterior, 5.8 mm ventral, and 2.3 mm lateral to the bregma). The needle was left in place for 15 min, and then slowly withdrawn. Surgical control rats received 2 μl of saline only. The hole was sealed with bone wax, and the skin incision was closed using sutures.

The vehicles received 1 % carboxymethyl cellulose orally (0.5 ml, twice a day) by gavage. Deferiprone and clioquinol oral solution was made fresh before each gavage. Deferiprone (dissolved in 0.5 ml saline according to administration dosage, twice a day) and clioquinol (dissolved in 0.5 ml 1 % carboxymethyl cellulose according to administration dosage, twice a day) were administered at 24 h after ICH.

Behavioral Tests

Garcia scores were used to evaluate neurological deficits before rats were sacrificed at each time point [15]; the score given to each rat at the completion of the evaluation is the summation of all six individual test scores. Six items were measured: spontaneous activity, symmetry of movements, forepaw outstretching, climbing, body proprioception, and vibrissae touch. According to the degree of deficit, the animals were scored from 0 to 3 in the first three items and 1 to 3 in the last items. All behavioral tests were conducted by the same investigator, who was blind to the experiment.

Measurement of Brain Water Content

Brain water content was measured via the wet-weight/dry-weight method, as described previously [16]. Briefly, animals were sacrificed by decapitation under deep pentobarbital anesthesia after the neurological behavioral scoring; brains were quickly removed and divided into 4-mm thick sections. All specimens obtained from ipsilateral basal ganglion were weighed on an analytical microbalance (APX-60, Denver Instrument, Bohemia, NY) immediately, as well as after drying (100 °C for 48 h). Brain water content was calculated as percentage of (wet weight–dry weight)/wet weight × 100 [17].

Iron Staining

Sections were stained with Perls' Prussian blue to locate ferric ion (Fe^{3+}) deposits. Briefly, sections were rinsed in distilled water and immersed in Pearl's solution (1 % potassium ferrocyanide and 1 % HCl (*v*/*v*)) for 20 min. Sections were then rinsed with distilled water, and counter stained with nuclear-fast red dyeing for 5 min [16].

Total Iron Contents in the Brain

One hundred-milligram of brain tissue around hematoma was wet-digested with 4 mL concentrated nitric acid (HNO_3) and the residue brought to 4.0 mL with 0.1 m/L HNO_3. Total brain iron concentration (μg/g of tissue; wet weight) was measured by flame atomic absorption spectrometry (TAS-990, Beijing PUXI General Instrument, China) according to standard protocol [18].

ROS Contents

For analysis of ROS in brain tissues, the redox-sensitive fluorescent probe dichloro-dihydro-fluorescein diacetate (DCFH-DA) was used according to ROS assay kit (Beyotime, Inc., Shanghai, China). The brain homogenate was diluted 1:20 (*v*/*v*) with ice-cold Locke's buffer (154 mM NaCl, 5.6 mM KCl, 3.6 mM $NaHCO_3$, 2.0 mM $CaCl_2$, 10 mM D-glucose, and 5 mM HEPES, pH 7.4) to obtain a concentration of 10 mg tissue/ml. The reaction mixture (1 ml) containing Locke's buffer (pH 7.4), 0.2 ml homogenate, and 10 μl of DCFH-DA (5 mM) was incubated for 30 min at room temperature. Fluorescent intensity for the conversion of DCFH-DA to fluorescent product DCF was analyzed at 485 nm excitation and 535 nm emission using a fluorescence spectrophotometer. ROS was quantified from a DCF standard curve and data are expressed as picomole per minute per milligram protein [19].

Immunohistochemical Analysis

Embedded brain tissue was cut into 4-μm thick sections. Dewaxed and hydrated sections were treated with 3 % hydrogen peroxide in 100 mM phosphate-buffered saline (PBS), and non-specific protein binding were blocked by incubation with 10 % normal goat serum in PBS for 20 min at 37 °C. Sections were incubated with the anti-ferritin (1:200), transferrin (Tf, 1:200), CD71 (transferrin receptor (TfR), 1:200), and divalent metal transporter 1 (DMT1, 1:400); these primary antibodies were purchased from Wuhan Boster Biotech Co., China; and anti-ferroportin (Fpn, 1:100; Bo Orson Biotech Co., Beijing, China) at 4 °C overnight. Primary antibodies were rinsed and reacted with biotinylated secondary antibodies in PBS-blocking buffer at 37 °C for 20 min, and visualized by SABC (SABC Elite kit; Wuhan Boster Biotech Co., China) and DAB reagent (Beijing Zhongshan Jinqiao Biotech Co., China). Sections were mounted and the images were analyzed with an Olympus BX51 microscope equipped with a DP71 camera and DP-B software (Olympus Co., Japan). Immuno-positive cells were identified in the perihematomal area, which was observed at the same location in all specimens by one investigator who was blind to the grouping.

Real-Time Quantitative Polymerase Chain Reaction

Total RNA was extracted from brain tissues stored at −80 °C by using TRIzol Reagent (Sigma-Aldrich, USA) in accordance with the manufacturer's instructions. Complementary DNA was reverse transcribed by using a two-step RT-PCR kit (Takara Bio, China). RT-qPCR analysis was performed using ABI7300 System SDS RQ Study Software (Life Technologies, USA) with the SYBR green RT-PCR Kit (Takara Bio, China). A 20-μL total reaction mixture volume was used in the PCR; this contained 8 μL of diluted complementary DNA reaction products, 10 μL of SYBR green PCR Master Mix, and 2 μL of forward and reverse primers. Reaction conditions were as follows: initial denaturation at 95 °C for 2 min, 40 cycles of denaturation at 95 °C for 30 s, and annealing and elongation at 60 °C for 45 s. Reverse transcription was performed in triplicate. To standardize ferritin, Tf/TfR, DMT1, and Fpn mRNA concentration, transcript levels of the housekeeping gene β-actin were determined in parallel for each sample. Final results were expressed as the copy ratio of β-actin transcripts. The amount of target was calculated by the $2-\Delta\Delta Ct$ method [20].

Statistical Analysis

Statistical analysis was performed using SPSS 17.0 (SPSS, Armonk, NY). Data were expressed as a mean±standard division (SD). P value <0.05 was considered statistically significant. Results were compared among groups using a Dunnett's T3 multiple comparison test.

Results

Effect of Deferiprone and Clioquinol on Survival of Animals

Administration of deferiprone at dose of 200 mg/kg [21] for 3–5 days caused significant mortality (n=6) in this study; therefore, we choose deferiprone of 125 mg/kg for further study. Clioquinol in high dosage was more effective in improving neurological behavior and reducing brain water content, so we choose clioquinol of 100 mg/kg/day for further

study. Neither ICH group nor clioquinol group caused significant mortality in this study.

Effect of Deferiprone and Clioquinol on ICH Induced Neurological Deficits

At day 2, 3, and 7 after surgery, we observed significant neurological deficits (Garcia scores) in all vehicle and deferiprone-treated ICH rats, compared with sham group ($^{\#}p<0.05$ vs. sham). Clioquinol ameliorated ICH-induced neurological deficits at day 2, 3, and 7 after surgery ($*p<0.05$ vs. vehicle and $p<0.05$ vs. deferiprone; Fig. 1). A similar effect was not shown with deferiprone in this study. At day 14 after surgery, we observed significant neurological recovery in all ICH animals (with or without treatment).

Effect of Deferiprone and Clioquinol on ICH Induced Brain Edema

At day 2 and 3 after surgery, brain water content was enhanced in all vehicle and deferiprone-treated ICH rats, compared with sham-operated animals ($^{\#}p<0.05$ vs. sham). Clioquinol reduced ICH-induced brain edema at day 2 and 3 after surgery ($*p<0.05$ vs. vehicle and $p<0.05$ vs. deferiprone; Fig. 1); at day 7 and 14 after surgery, we observed brain edema attenuate in all ICH animals (with or without treatment).

Effect of Deferiprone and Clioquinol on ROS Formation After ICH

ROS production was prominently increased in ICH rats (with or without treatment), compared with sham-operated animals ($^{\#}p<0.05$ vs. sham). Only clioquinol reduced ICH-induced ROS production ($*p<0.05$ vs. vehicle and $p<0.05$ vs. deferiprone; Fig. 1).

Effect of Deferiprone and Clioquinol on Iron Deposits Following ICH

All ICH animals (with or without treatment) showed markedly increased iron deposits, compared with sham-operated animals ($^{\#}p<0.05$ vs. sham). Both deferiprone and clioquinol decreased ICH-induced iron deposits ($*p<0.05$ vs. vehicle; Fig. 2). Iron deposits reached a peak at day 7 after ICH.

Effect of Deferiprone and Clioquinol on Ferritin Expression After ICH

Ferritin was mainly expressed in cytoplasm of neuroglia and neurons. As a form of iron stores, ferritin expression

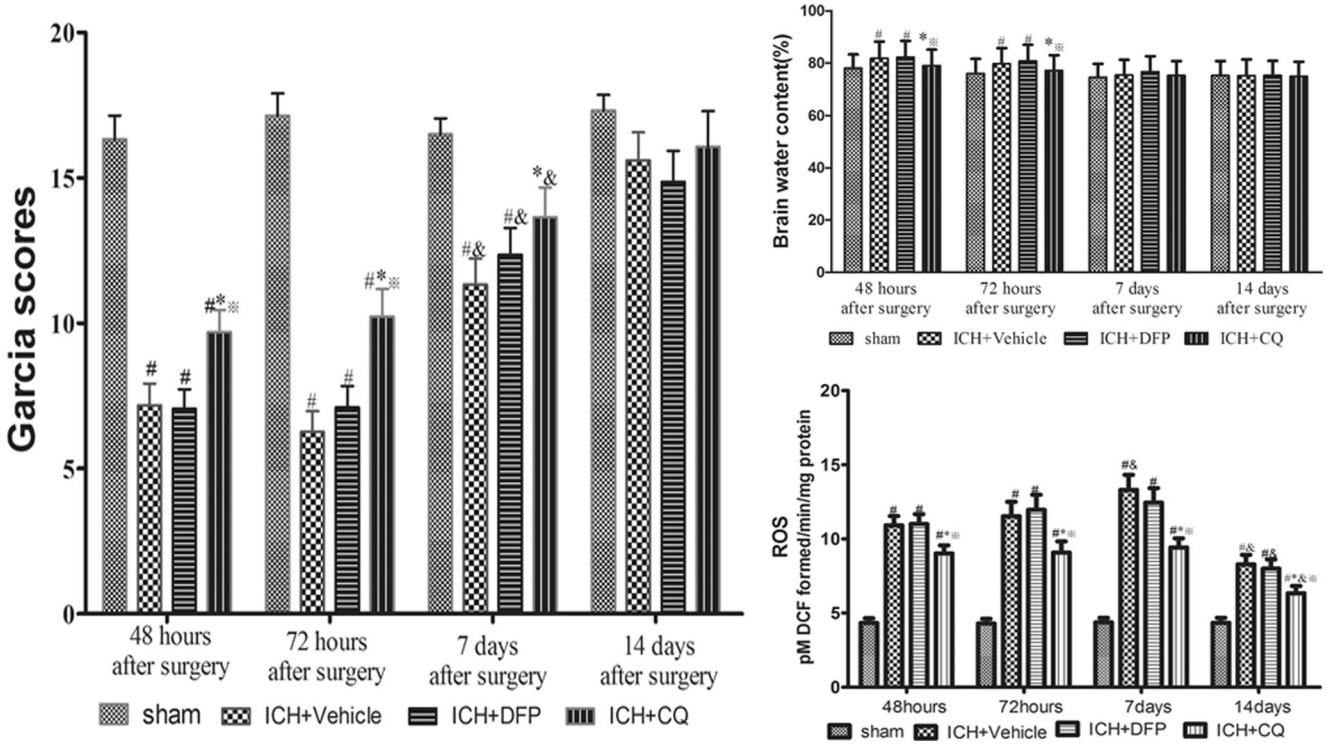

Fig. 1 Comparison of the results from Garcia scores, brain water content, and ROS in four groups (sham, vehicle, deferiprone, and clioquinol); $\#p<0.05$ vs. sham; $*p<0.05$ vs. vehicle; $p<0.05$ vs. deferiprone; and $p<0.05$ vs. former point by Dunnett's T3 multiple comparison test

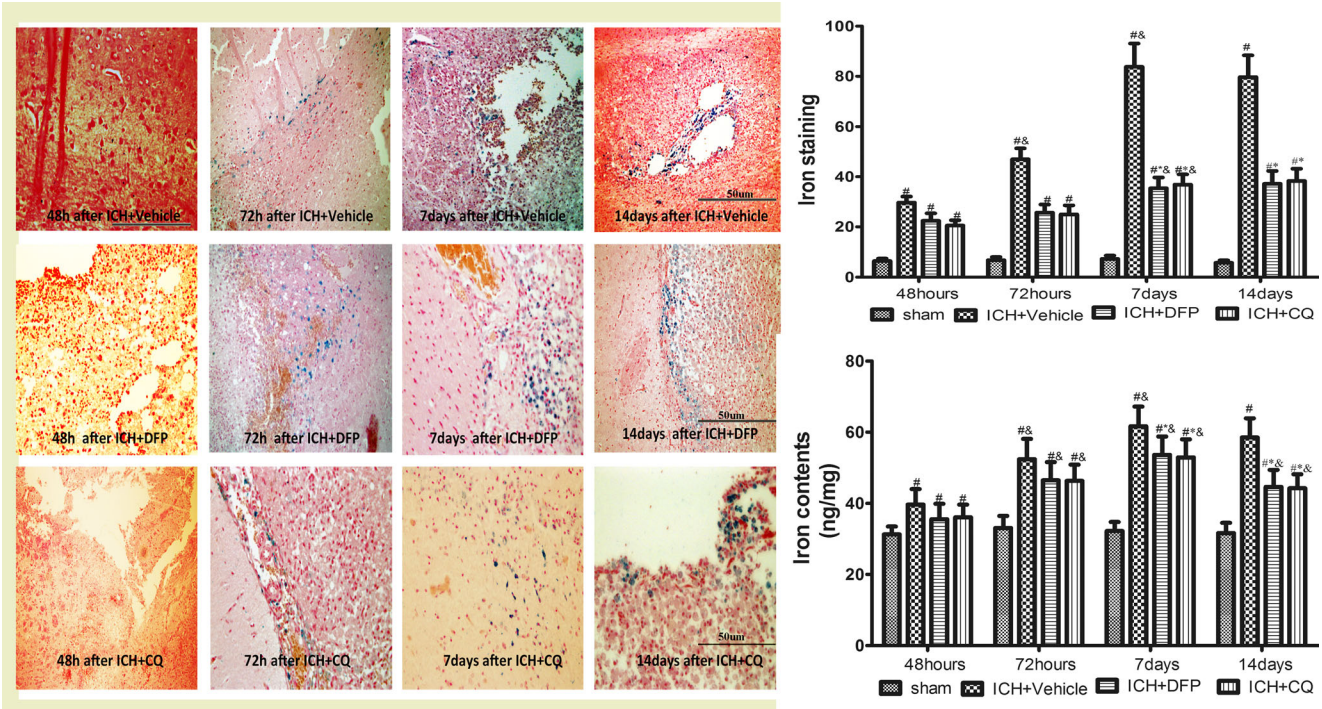

Fig. 2 Iron staining (*blue spot*) were shown around hematoma. Comparison of the results from iron staining and brain iron contents at different time point in four groups (sham, vehicle, deferiprone, and clioquinol); #$p<0.05$ vs. sham; *$p<0.05$ vs. vehicle; $p<0.05$ vs. deferiprone; and $p<0.05$ vs. former point by Dunnett's T3 multiple comparison test

was also enhanced after ICH (with or without treatment). Similar to iron deposits, ferritin expression reached a plateau at day 7, and both iron chelators could reduce ferritin expression. Interestingly, clioquinol reduced more mRNA of ferritin than deferiprone at day 3, 7, and 14 after surgery (Fig. 3).

Effect of Deferiprone and Clioquinol on Transferrin Expression After ICH

Transferrin was mostly expressed in the cytoplasm of neuroglia, and a small amount expressed in neurons after ICH. The data showed that transferrin was significantly increased in

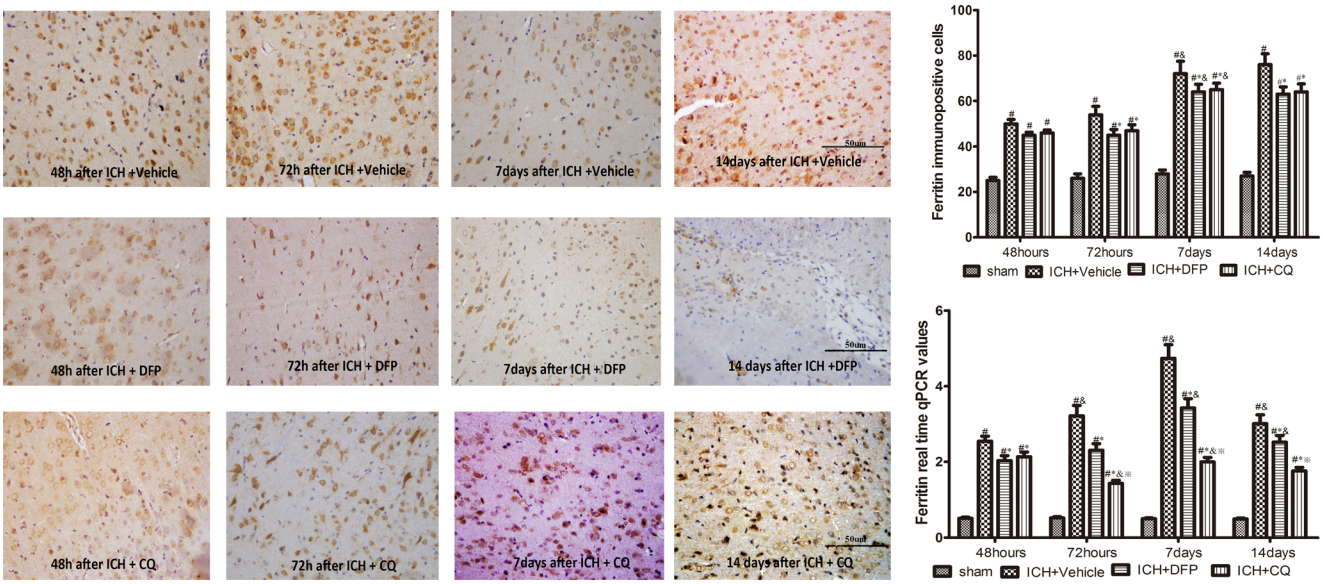

Fig. 3 Ferritin immuno-positive cells (*brown*) were shown after operation. It is mainly expressed in cytoplasm of neuroglia and neurons. Comparison of the results from ferritin immunostaining and RT-qPCR production in four groups (sham, vehicle, deferiprone, and clioquinol); #$p<0.05$ vs. sham; *$p<0.05$ vs. vehicle; $p<0.05$ vs. deferiprone; and $p<0.05$ vs. former point by Dunnett's T3 multiple comparison test

ICH (with or without treatment), compared with sham-operated animals ($^{\#}p<0.05$ vs. sham). Both deferiprone and clioquinol enhanced ICH-induced transferrin expression ($*p<0.05$ vs. vehicle; Fig. 4). Transferrin reached a peak at day 3 in mRNA level and at day 7 in immunohistochemistry after ICH. Surprisingly, the results showed that clioquinol amplified transferrin expression at day 7 and 14 in immunohistochemistry and at day 3, 7, and 14 in mRNA, compared with deferiprone treatment.

Effect of Deferiprone and Clioquinol on Transferrin Receptor Expression After ICH

Transferrin receptor was primarily expressed in the cytoplasm of neuroglia and neurons, but a few was found at the membrane of endothelia, this is consistent with its role for transporting iron. Similar to transferrin, the results showed that transferrin receptor was significantly increased after ICH (with or without treatment), compared with sham-operated animals ($^{\#}p<0.05$ vs. sham). Both deferiprone and clioquinol enhanced ICH-induced transferrin receptor expression at day 3 and 7 in immunohistochemistry and at day 3, 7, and 14 in mRNA after surgery ($*p<0.05$ vs. vehicle; Fig. 5). Transferrin receptor reached a plateau at day 3 after ICH. Same as transferrin, clioquinol amplified transferrin receptor expression at day 3 and 7 after surgery, compared with deferiprone treatment. At day 14 after surgery, the transferrin receptor expression was receded.

Effect of Deferiprone and Clioquinol on DMT1 Expression After ICH

As shown in Fig. 6, DMT1 expression was principal in cytoplasm of neurons, some were at glia and a few were at endothelial cells. Similar to the other iron transporters, all animals showed DMT1 expression significantly increased in ICH, compared with sham-operated animals. Deferiprone enhanced ICH-induced DMT1 expression at day 3 in immunohistochemistry and at day 2, 3, and 7 in mRNA after surgery ($*p<0.05$ vs. vehicle; Fig. 6). DMT1 reached a plateau at day 7 after ICH. Different from ferric iron transporters, clioquinol weakened DMT1 expression at day 3, 7, and 14 after surgery in immunohistochemistry and all the time in mRNA, compared with deferiprone treatment.

Effect of Deferiprone and Clioquinol on Ferroportin Expression After ICH

As shown in Fig. 7, Fpn expression was mainly at the membrane of endothelial cells which is consistent with its role for iron exportation from the brain, the other located at glia. Same as DMT1, all animals showed Fpn expression significantly increased in ICH (with or without treatments), compared with

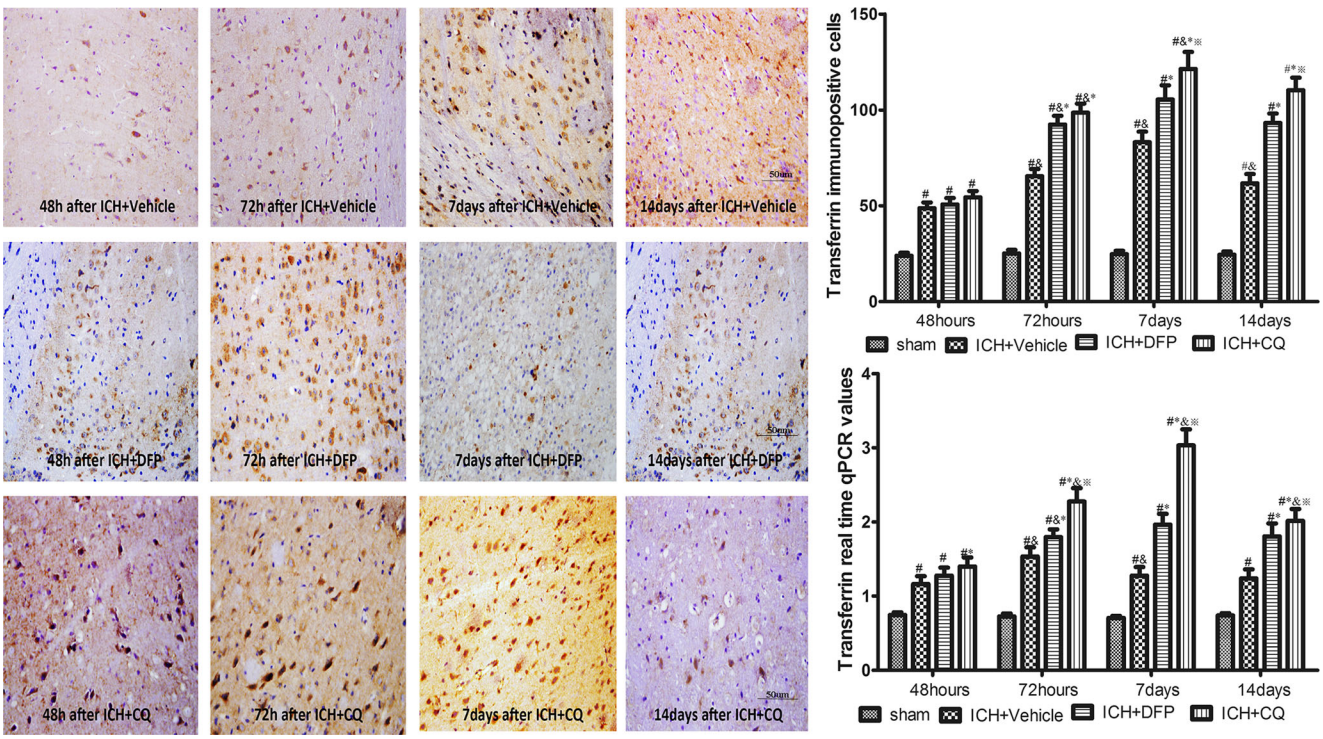

Fig. 4 Localization of transferrin by immunohistochemistry method (*brown*). Comparison of the results from transferrin immunostaining and RT-qPCR production in four groups (sham, vehicle, deferiprone, and clioquinol); $\#p<0.05$ vs. sham; $*p<0.05$ vs. vehicle; $p<0.05$ vs. deferiprone; and $p<0.05$ vs. former point by Dunnett's T3 multiple comparison test

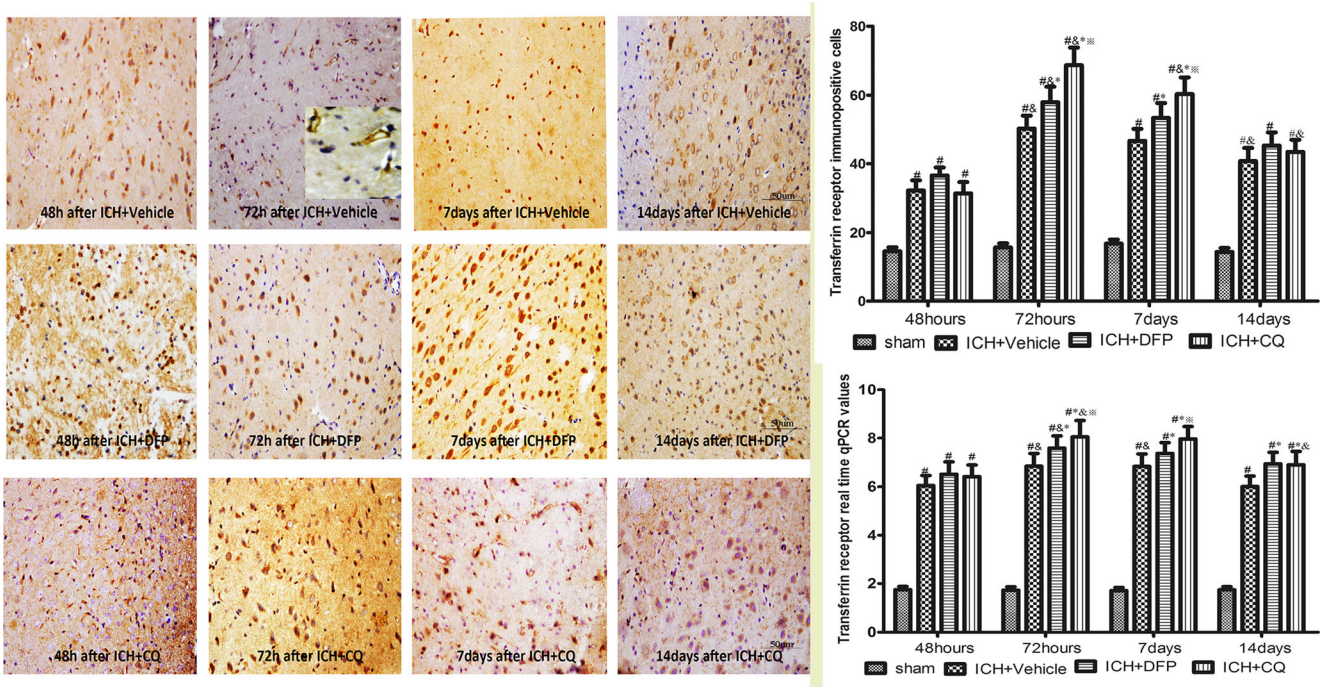

Fig. 5 Localization of transferrin receptor by immunohistochemistry method (*brown*). Comparison of the results from transferrin receptor immunostaining and RT-qPCR production in four groups (sham, vehicle, deferiprone, and clioquinol); #$p<0.05$ vs. sham; *$p<0.05$ vs. vehicle; $p<0.05$ vs. deferiprone; and $p<0.05$ vs. former point by Dunnett's T3 multiple comparison test

sham-operated animals. But just clioquinol enhanced ICH-induced Fpn expression at day 7 and 14 in immunohistochemistry and at all time points in PCR after surgery (*$p<0.05$ vs. vehicle; Fig. 7); deferiprone had no role on Fpn compared with vehicle group. Clioquinol enhanced Fpn expression compared with deferiprone treatment group ($p<0.05$ vs. deferiprone).

Discussion

In this study, we found that ICH induced iron accumulation, brain edema, ROS formation, and neurological deficits. Clioquinol improved neurological outcome probably through reducing brain edema and ROS production. Deferiprone reduced iron contents but not brain edema and ROS, and it failed

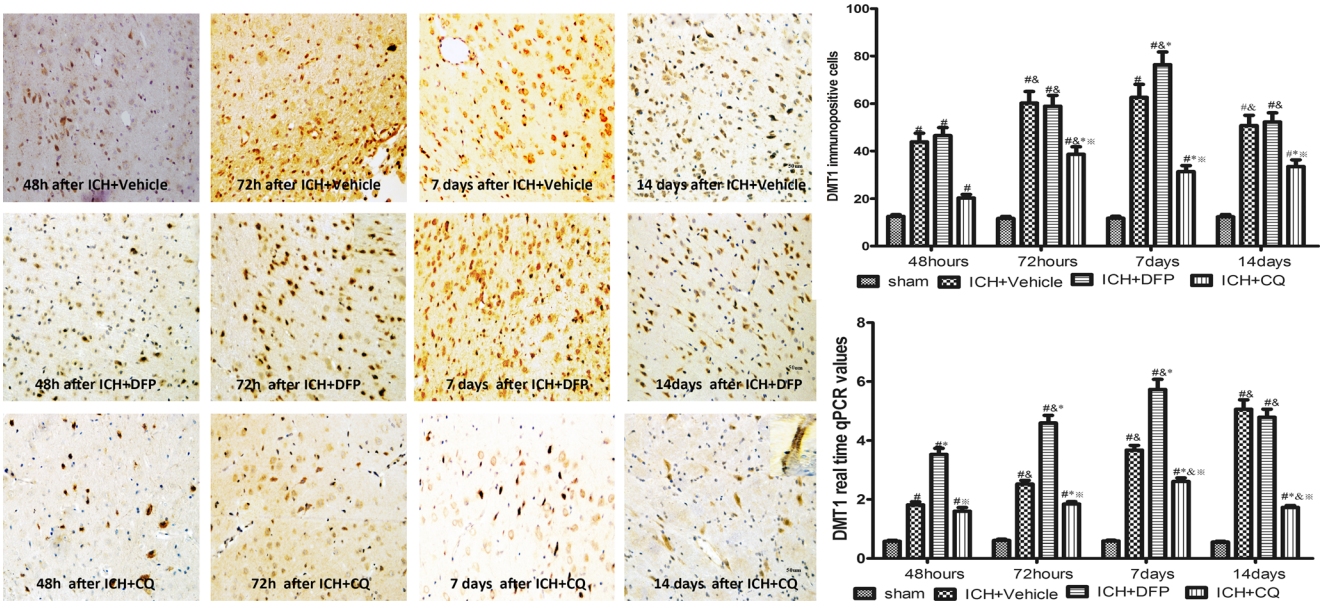

Fig. 6 Localization of divalent metal transporter 1 (DMT1) by immunohistochemistry method (*brown*). Comparison of the results from DMT1 immunostaining and RT-qPCR production in four groups (sham, vehicle, deferiprone, and clioquinol); #$p<0.05$ vs. sham; *$p<0.05$ vs. vehicle; $p<0.05$ vs. deferiprone; and $p<0.05$ vs. former point by Dunnett's T3 multiple comparison test

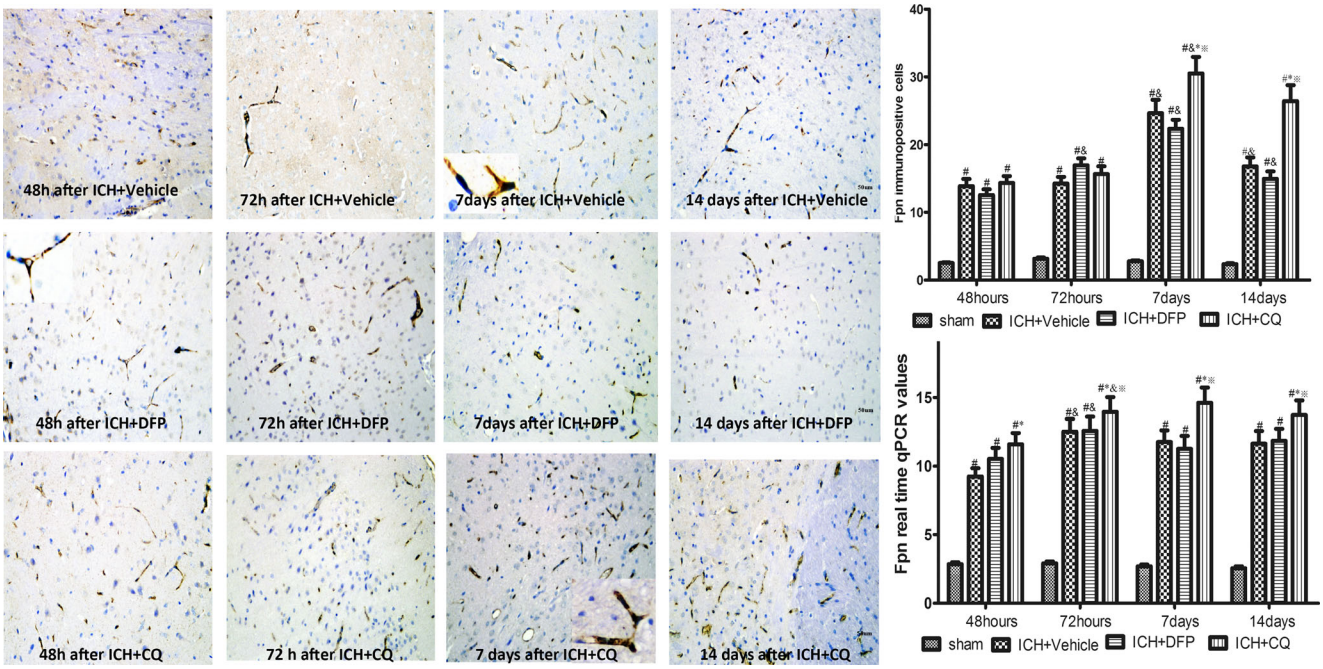

Fig. 7 Localization of ferroportin (Fpn) by immunohistochemistry method (*brown*). Comparison of the results from Fpn immunostaining and RT-qPCR production in four groups (sham, vehicle, deferiprone, and clioquinol); #$p<0.05$ vs. sham; *$p<0.05$ vs. vehicle; $p<0.05$ vs deferiprone; and $p<0.05$ vs. former point by Dunnett's T3 multiple comparison test

to improve the outcome. ICH initiated endogenous iron chelators and transporters, both exogenous iron chelators (Fe^{2+}/Fe^{3+}) enhanced transferrin and transferrin receptor, clioquinol seems to have more powerful effect on them compared with DFP. Clioquinol enhanced expression of Fpn but not DMT1, deferiprone enhanced expression of DMT1 but not Fpn.

The peak coincidence of iron storage and ROS in our study confirmed that iron was probably the primary cause of ROS production, and Fenton reaction was probably the major mechanism, causing lipid peroxidation and neuronal injury in the brain [9, 22]. Ferritin as another main iron binding protein, its primary role is against iron toxicity that involves oxidative damage with mitochondrial involvement. Ferritin iron may have a pro-oxidant role under pathological conditions. This indicates that under conditions in which ferritin iron capacity to store iron is overwhelmed or impaired by either chemical or genetic reasons, ferritin iron can contribute to tissue damage [23, 24]. We found that major ferritin expressed in cytoplasm of neuroglia and neurons. Increased iron levels within the cytoplasm of vulnerable neurons suggest that this may also be an important site of oxidative activity. It showed that intracellular, rather than extracellular chelation of ferrous or ferric iron may be more effective in reducing hydroxyl radical-induced cell damage and cell viability [25]. Meanwhile, brain edema and Garcia scores showed the most deterioration at day 2 and 3, which was out of step with iron accumulation. So there are other detrimental factors such as mass effect, thrombin, and inflammation involved in the edema formation; moreover, it needs other more specialized scale scores to evaluate the neurological deficits on the long outcome.

It is known that the redox-active form of iron, ferrous iron, is neurotoxic due to the generation of ROS by the Fenton reaction [24]. Fe^{2+} may play a potent role in the pathogenesis of secondary insult following ICH. Fe^{2+} is oxidized to Fe^{3+} by hydrogen peroxide, forming a hydroxyl radical and a hydroxide ion in the process. Fenton reaction is as follows [26]: $Fe^{2+}+H_2O_2 \rightarrow Fe^{3+}+HO\bullet+OH–$; as shown in the equation, chelating ferrous iron will reduce oxidative free radical formation, but chelating the ferric iron would facilitate the reaction process and possibly increase the free radical production. Fe^{2+} binding may attenuate oxidative stress and inhibit Fe^{2+}-induced lipid peroxidation from iron overload. On the other hand, H_2O_2 can significantly increase the intracellular free radicals, leading to serious DNA damage and significantly reduce superoxide dismutase, glutathione peroxidase, catalase, and lipase activity [27]. So ferrous iron chelator—clioquinol—may prevent its happening and reduce brain edema, but it would not happen with ferric iron chelator—deferiprone. Furthermore, existing data showed that hydrophilic ferrous or ferric chelators and lipophilic ferric chelators were essentially ineffective in preventing cellular NAD(+) depletion when added at physiological concentrations [25]. But lipophilic ferrous chelators, due to their actions inside the cells, are effective agents for moderating neuronal damage in conditions such as Alzheimer's disease (AD), where intracellular oxidative stress plays a significant role in disease pathology. As the intracellular environment is a major site of

oxidative damage, effective targeting of the specific site of free radical generation by selected chelation drugs may be helpful in reducing non-specific side effects, and thus provide a more effective therapy [25]. Clioquinol has the capacity to bind both extracellular and intracellular ferrous iron [25]. Its ability to chelate intracellular iron resulted in a decrease in intracellular OH• mediated damage [25]. In the 1970s, clioquinol was linked to an outbreak of subacute myelo-optic neuropathy in Japan [28] and was banned in many countries. Subsequent epidemiologic analysis questioned the link between subacute myelo-optic neuropathy and clioquinol [29], and it remains available in several countries, including Canada, where it is sold in a topical preparation. Clioquinol was then moved into clinical trials for patients with AD [30, 31]. It proved nontoxic in a small Swedish trial [30] and a larger trial conducted in Australia [31]. We observed that deferiprone had greater possibility of unexpected side effects than clioquinol. Clioquinol, a ferrous iron chelator had a beneficial effect on ICH but not ferric iron chelator (deferiprone), and showed that Fe^{2+} probably was the key factor in the pathophysiology of ICH. Fe^{2+} binding may attenuate some ROS consequences from iron overload.

With iron accumulation in the brain after ICH, iron-related transport proteins were activated to keep the iron homeostasis in the brain. Iron homeostasis in cells is regulated by interactions of proteins involved in iron uptake, release, and storage [32]. Ferritin, transferrin, transferrin receptor, DMT1, and ferroportin were all involved in the iron-regulating process. Our results showed that all the iron-related chelating and transport proteins mentioned above increased after ICH. Traditionally, transferrin-mediated transport system has been considered as the primary mechanism for cellular iron delivery and identified in the BBB [33]. Our results showed that transferrin receptors reached the plateau earlier than transferrin, suggested the receptor was possibly earlier in the adaptation to iron overload in the brain. The enhanced expression of Tf/TfR was probably associated with the iron egress accompanied by iron accumulation in the brain after ICH. Plasma transferrin is a powerful ferric endogenous chelator, capable of binding iron tightly but reversibly. A molecule of Tf can bind two atoms of ferric iron with high affinity. It facilitates regulated iron transport and cellular uptake, and it maintains Fe^{3+} in a redox-inert state, preventing the generation of toxic free radicals [34]. There are both transferrin and non-transferrin-dependent systems for iron delivery to the brain and that the preference for one pathway over another appears to be dependent on the iron status of the endothelial cells [34]. DMT1 is the major mediator for Fe^{2+} influx, pre-treatment with DMT1 inhibitor—ebselen—significantly reduces the iron-transporting activity of DMT1 and inhibits ROS generation [35]. Fpn is the only known molecule to export Fe^{2+} from neuronal cells. Fpn has been identified in the brain microvascular endothelial cells of the blood-brain barrier. Our staining results verified and suggested that its location was related to iron exporter function. Fpn controls iron efflux from neurons and iron transport across the basolateral membrane of endothelial cells of the BBB [36]. In this study, we found that expression of DMT1 and Fpn were increased in ICH; they all involved in the iron regulation when iron overload occurred in the brain after ICH.

So what is the effect of the exogenous iron chelators on endogenous iron chelators and regulators in ICH? We found that both iron chelators upregulated the expression of transferrin and transferrin receptor, they all accelerated iron trafficking after ICH, but clioquinol seems to have a stronger effect on them. Both iron chelators played different role on the Fe^{2+} transporters. Ferroportin, the only channel for iron export, its downregulation led to iron accumulation and dopaminergic neurons' degeneration [37] and aggravated ROS generation in PD [38]. As mentioned before, DMT1 inhibitor significantly inhibited ROS generation [35]. The neuroprotective effect of clioquinol probably facilitates iron export through strengthening expression of Fpn and reducing expression of DMT1. But for deferiprone, while it enhanced DMT1 and appeared no role for Fpn, it seemed to have little effect on outcome of rat ICH.

Conclusion

Ferrous iron may play a key role in the pathogenesis of secondary injury after ICH. Fe^{2+} binding may attenuate some ROS consequences from iron overload then mitigate brain edema. Exogenous iron chelator functioned by affecting endogenous iron chelators or transporters. Clioquinol improved neurological outcome of rat ICH probably through reducing brain edema and ROS production, it facilitated Fe^{2+} export and inhibited Fe^{2+} import through enhancing Fpn and reducing DMT1 expression. DFP failed to improve the outcome probably owing to its upregulation for DMT1 but nothing to Fpn, so DFP seemed to have little effect on brain edema and ROS.

Acknowledgments This work was supported by the Shanxi provincial Science and Technology Agency (2014011041-5) and Shanxi provincial Hygiene Department (201301010).

References

1. Babu R, Bagley JH, Di C, Friedman AH, Adamson C (2012) Thrombin and hemin as central factors in the mechanisms of intracerebral hemorrhage-induced secondary brain injury and as potential targets for intervention. Neurosurg Focus 32:E8
2. Aronowski J, Zhao X (2011) Molecular pathophysiology of cerebral hemorrhage: secondary brain injury. Stroke 42:1781–1786

3. Gu Y, Hua Y, He Y, Wang L, Hu H, Keep RF et al (2011) Iron accumulation and DNA damage in a pig model of intracerebral hemorrhage. Acta Neurochir Suppl 111:123–128
4. Hatakeyama T, Okauchi M, Hua Y, Keep RF, Xi G (2013) Deferoxamine reduces neuronal death and hematoma lysis after intracerebral hemorrhage in aged rats. Transl Stroke Res 4:546–553
5. Pérez de la Ossa N, Sobrino T, Silva Y, Blanco M, Millán M, Gomis M et al (2010) Iron-related brain damage in patients with intracerebral hemorrhage. Stroke 41:810–813
6. Caliaperumal J, Wowk S, Jones S, Ma Y, Colbourne F (2013) Bipyridine, an iron chelator, does not lessen intracerebral iron-induced damage or improve outcome after intracerebral hemorrhagic stroke in rats. Transl Stroke Res 4:719–728
7. Xie Q, Gu Y, Hua Y, Liu W, Keep RF, Xi G (2014) Deferoxamine attenuates white matter injury in a piglet intracerebral hemorrhage model. Stroke 45:290–292
8. Auriat AM, Silasi G, Wei Z, Paquette R, Paterson P, Nichol H et al (2012) Ferric iron chelation lowers brain iron levels after intracerebral hemorrhage in rats but does not improve outcome. Exp Neurol 234:136–143
9. Atamna H, Frey WH 2nd (2004) A role for heme in Alzheimer's disease: heme binds amyloid beta and has altered metabolism. Proc Natl Acad Sci U S A 101:11153–11158
10. Chun HJ, Kim DW, Yi HJ, Kim YS, Kim EH, Hwang SJ et al (2012) Effects of statin and deferoxamine administration on neurological outcomes in a rat model of intracerebral hemorrhage. Neurol Sci 33:289–296
11. Warkentin LM, Auriat AM, Wowk S, Colbourne F (2010) Failure of deferoxamine, an iron chelator, to improve outcome after collagenase-induced intracerebral hemorrhage in rats. Brain Res 1309:95–103
12. Kontoghiorghes GJ, Efstathiou A, Kleanthous M, Michaelides Y, Kolnagou A (2009) Risk/benefit assessment, advantages over other drugs and targeting methods in the use of deferiprone as a pharmaceutical antioxidant in iron loading and non-iron loading conditions. Hemoglobin 33:386–397
13. Abbruzzese G, Cossu G, Balocco M, Marchese R, Murgia D, Melis M et al (2011) A pilot trial of deferiprone for neurodegeneration with brain iron accumulation. Haematologica 96:1708–1711
14. Prachayasittikul V, Prachayasittikul S, Ruchirawat S, Prachayasittikul V (2013) 8-Hydroxyquinolines: a review of their metal chelating properties and medicinal applications. Drug Des Devel Ther 7:1157–1178
15. Garcia JH, Wagner S, Liu KF, Hu XJ (1995) Neurological deficit and extent of neuronal necrosis attributable to middle cerebral artery occlusion in rats. Statistical validation. Stroke 26:627–634
16. Jolkkonen J, Jokivarsi K, Laitinen T, Gröhn O (2007) Subacute hemorrhage and resolution of edema in Rose Bengal stroke model in rats coincides with improved sensorimotor functions. Neurosci Lett 428:99–102
17. Shao A, Wang Z, Wu H, Dong X, Li Y, Tu S, Tang J, Zhao M et al (2014) Enhancement of autophagy by histone deacetylase inhibitor trichostatin A ameliorates neuronal apoptosis after subarachnoid hemorrhage in rats. Mol Neurobiol 2014 Nov 18
18. Prohaska JR, Gybina AA (2005) Rat brain iron concentration is lower following perinatal copper deficiency. J Neurochem 93: 698–705
19. Chen S, Ren Q, Zhang J, Ye Y, Zhang Z, Xu Y et al (2014) N-acetyl-L-cysteine protects against cadmium-induced neuronal apoptosis by inhibiting ROS-dependent activation of Akt/mTOR pathway in mouse brain. Neuropathol Appl Neurobiol 40:759–777
20. Livak KJ, Schmittgen TD (2001) Analysis of relative gene expression data using real-time quantitative PCR and the 2(-Delta DeltaC(T)) method. Methods 25:402–408
21. Iranmanesh M, Fatemi SJ, Ebrahimpour R, Dahooee Balooch F (2013) Chelation of chromium(VI) by combining deferasirox and deferiprone in rats. Biometals 26:465–471
22. Markesbery WR (1997) Oxidative stress hypothesis in Alzheimer's disease. Free Radic Biol Med 23:134–147
23. Arosio P, Levi S (2010) Cytosolic and mitochondrial ferritins in the regulation of cellular iron homeostasis and oxidative damage. Biochim Biophys Acta 1800:783–792
24. Reif DW (1992) Ferritin as a source of iron for oxidative damage. Free Radic Biol Med 12:417–427
25. Jayasena T, Grant RS, Keerthisinghe N, Solaja I, Smythe GA (2007) Membrane permeability of redox active metal chelators: an important element in reducing hydroxyl radical induced NAD+ depletion in neuronal cells. Neurosci Res 57:454–461
26. Lemire JA, Harrison JJ, Turner RJ (2013) Antimicrobial activity of metals: mechanisms, molecular targets and applications. Nat Rev Microbiol 11:371–384
27. Cai X, Chen X, Wang X, Xu C, Guo Q, Zhu L et al (2013) Preprotective effect of lipoic acid on injury induced by H_2O_2 in IPEC-J2 cells. Mol Cell Biochem 378:73–78
28. Tsubaki T, Honma Y, Hoshi M (1971) Neurological syndrome associated with clioquinol. Lancet 1:696–697
29. Meade TW (1975) Subacute myelo-optic neuropathy and clioquinol. An epidemiological case-history for diagnosis. Br J Prev Soc Med 29:157–169
30. Regland B, Lehmann W, Abedini I, Blennow K, Jonsson M, Karlsson I et al (2001) Treatment of Alzheimer's disease with clioquinol. Dement Geriatr Cogn Disord 12:408–414
31. Ritchie CW, Bush AI, Mackinnon A, Macfarlane S, Mastwyk M, MacGregor L et al (2003) Metal-protein attenuation with iodochlorhydroxyquin (clioquinol) targeting abeta amyloid deposition and toxicity in Alzheimer disease: a pilot phase 2 clinical trial. Arch Neurol 60:1685–1691
32. Kühn LC (2015) Iron regulatory proteins and their role in controlling iron metabolism. Metallomics 7:232–243
33. Jefferies WA, Brandon MR, Hunt SV, Williams AF, Gatter KC, Mason DY (1984) Transferrin receptor on endothelium of brain capillaries. Nature 312:162–163
34. Gkouvatsos K, Papanikolaou G, Pantopoulos K (2012) Regulation of iron transport and the role of transferrin. Biochim Biophys Acta 1820:188–202
35. Xie L, Zheng W, Xin N, Xie JW, Wang T, Wang ZY (2012) Ebselen inhibits iron-induced tau phosphorylation by attenuating DMT1 up-regulation and cellular iron uptake. Neurochem Int 61:334–340
36. Li L, Li YW, Zhao JY, Liu YZ, Holscher C (2009) Quantitative analysis of iron concentration and expression of ferroportin 1 in the cortex and hippocampus of rats induced by cerebral ischemia. J Clin Neurosci 16:1466–1472
37. Zhang Z, Hou L, Song JL, Song N, Sun YJ, Lin X et al (2014) Pro-inflammatory cytokine-mediated ferroportin down-regulation contributes to the nigral iron accumulation in lipopolysaccharide-induced Parkinsonian models. Neuroscience 257:20–30
38. Song N, Wang J, Jiang H, Xie J (2010) Ferroportin 1 but not hephaestin contributes to iron accumulation in a cell model of Parkinson's disease. Free Radic Biol Med 48:332–341